Science of the Total Environment 837 (2022) 155802

Contents lists available at ScienceDirect

Science of the Total Environment

journal homepage: www.elsevier.com/locate/scitotenv

Updated trends for atmospheric mercury in the Arctic: 1995–2018

Katrina MacSween [a,*], Geoff Stupple [a], Wenche Aas [b], Katriina Kyllönen [c], Katrine Aspmo Pfaffhuber [b], Henrik Skov [d], Alexandra Steffen [a], Torunn Berg [e], Michelle Nerentorp Mastromonaco [f]

[a] Air Quality Processes Research Section, Air Quality Research Division, Science and Technology Branch Environment and Climate Change Canada, Government of Canada, Canada
[b] NILU – Norwegian Institute for Air Research, Instituttveien 18, 2027 Kjeller, Norway
[c] Finnish Meteorological Institute, Air Quality, Erik Palménin aukio 1, FI-00560 Helsinki, Finland
[d] Department of Environmental Science, iClimate, Aarhus University, Frederiksborgvej 399, 4000 Roskilde, Denmark
[e] Norwegian University for Technology and Science, Department of Chemistry, Høgskoleringen 5, 7491 Trondheim, Norway
[f] IVL Swedish Environmental Institute, Aschebergsgatan 44, 411 33 Gothenburg, Sweden

HIGHLIGHTS

- Annual mean TGM trends were negative for 8 of the 10 sites.
- Sub-Arctic sites generally showed greatest TGM decreases.
- High Arctic smallest overall TGM trend but increased from 1995–2018 to 2008–2018.
- High-arctic Hg speciation suggests changes to the gas-particle separation affecting deposition.

GRAPHICAL ABSTRACT

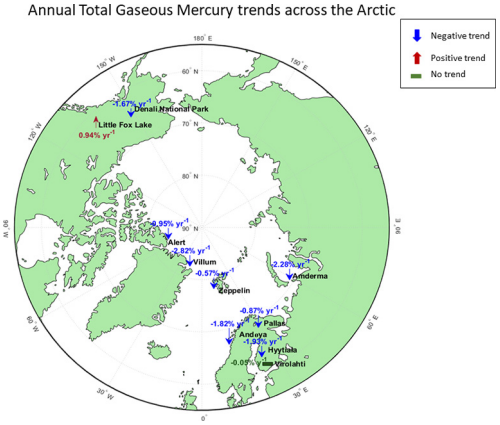

ARTICLE INFO

Editor: Christian Sonne

Keywords:
Mercury
Polar
Long-term
Sub-Arctic
TGM
GOM
PHg
Mann-Kendall

ABSTRACT

The Arctic region forms a unique environment with specific physical, chemical, and biological processes affecting mercury (Hg) cycles and limited anthropogenic Hg sources. However, historic global emissions and long range atmospheric transport has led to elevated Hg in Arctic wildlife and waterways. Continuous atmospheric Hg measurements, spanning 20 years, and increased monitoring sites has allowed a more comprehensive understanding of how Arctic atmospheric mercury is changing over time. Time-series trend analysis of TGM (Total Gaseous Mercury) in air was performed from 10 circumpolar air monitoring stations, comprising of high-Arctic, and sub-Arctic sites. GOM (gaseous oxidised mercury) and PHg (particulate bound mercury) measurements were also available at 2 high-Arctic sites. Seasonal mean TGM for sub-Arctic sites were lowest during fall ranging from 1.1 ng m^{-3} Hyytiälä to 1.3 ng m^{-3}, Little Fox Lake. Mean TGM concentrations at high-Arctic sites showed the greatest variability, with highest daily means in spring ranging between 4.2 ng m^{-3} at Amderma and 2.4 ng m^{-3} at Zeppelin, largely driven by local chemistry. Annual TGM trend analysis was negative for 8 of the 10 sites. High-Arctic seasonal TGM trends saw smallest decline during summer. Fall trends ranged from −0.8% to −2.6% yr^{-1}. Across the sub-Arctic sites spring showed the largest significant decreases, ranging between −7.7% to −0.36% yr^{-1}, while fall generally had no significant trends. High-Arctic speciation of GOM and PHg at Alert and Zeppelin showed that the timing and composition of atmospheric mercury deposition events are shifting. Alert GOM trends are increasing throughout the year, while PHg

* Corresponding author.
E-mail address: Katrina.macsween@ec.gc.ca (K. MacSween).

http://dx.doi.org/10.1016/j.scitotenv.2022.155802
Received 29 December 2021; Received in revised form 25 April 2022; Accepted 5 May 2022
Available online xxxx
0048-9697/Crown Copyright © 2022 Published by Elsevier B.V. This is an open access article under the CC BY license (http://creativecommons.org/licenses/by/4.0/).

trends decreased or not significant. Zeppelin saw the opposite, moving towards increasing PHg and decreasing GOM. Atmospheric mercury trends over the last 20 years indicate that Hg concentrations are decreasing across the Arctic, though not uniformly. This is potentially driven by environmental change, such as plant productivity and sea ice dynamics.

1. Introduction

Atmospheric mercury (Hg) is a hazardous toxin that exists on a global scale due to its unique chemistry and atmospheric processes. Mercury has a long atmospheric lifetime that allows it to be transported vast distances, such as to the remote environments of the Arctic (Driscoll et al., 2013; Sprovieri et al., 2010; Schroeder et al., 1998; Cobbett et al., 2007). Polar regions form unique environments with specific physical, chemical, and biological processes affecting pollutant cycles including that of Hg (Douglas et al., 2012). Atmospheric transport, riverine discharge, thawing permafrost, coastal erosion, atmospheric deposition and oceanic circulation form the key sources of Hg to the Arctic environment (Fisher et al., 2013; Zhang et al., 2015; DiMento et al., 2019; AMAP, 2011). Once deposited to a surface Hg can enter waterways, where it undergoes methylation and becomes a hazardous neurotoxin (Sunderland et al., 2009; Obrist et al., 2018; Selin et al., 2010). Deposited Hg may become available for methylation and subsequent bioaccumulation/biomagnification in food webs or it may be re-emitted to the atmosphere. Long-term monitoring of atmospheric Hg in the Arctic is crucial for assessing the sensitivity of the atmospheric input to changes in global mercury emissions, atmospheric circulation, and deposition (wet and dry) (Cole et al., 2013) and an important element in the assessment of the effectiveness of international regulatory efforts aiming to reduce Hg emissions and their effects, such as the global Minamata Convention on Mercury and Heavy Metals Protocol to the UNECE Convention on Long-Range Transboundary Air Pollution (CLRTAP).

The majority of Hg in the atmosphere is in the form of Gaseous Elemental Mercury (GEM), accounting for between 90 and 99% of all Hg, where it is estimated to be present for between 5 and 15 months (Horowitz et al., 2017; Goodsite et al., 2004, 2012; Skov et al., 2020; Saiz-Lopez et al., 2018; Selin, 2009). The other forms of Hg commonly found in the atmosphere are Gaseous Oxidised Mercury (GOM, also commonly called Reactive Gaseous Mercury, RGM) and Particulate-Bound Mercury (PHg, also commonly called PBM, HgP or PM). These species of Hg have a high deposition velocity causing them to be deposited close to production or emission sites, usually within hours (Brooks et al., 2006; Lindberg et al., 2002; Poissant et al., 2004; Landis et al., 2004). Atmospheric wet and dry deposition are an important pathway for Hg to the Arctic surface from the atmosphere, with deposition processes being altered by the unique Arctic conditions. Dry deposition is the air to surface flux of Hg in the absence of precipitation. All three phases of Hg (GEM, GOM, PHg) are able to undergo dry deposition (Lindberg et al., 2007; Brooks et al., 2006). However, GEM is the dominant form accounting for approximately 70% of all deposited Hg in the Arctic (Obrist et al., 2017). Dry deposition occurs all year round in polar regions, dominating during polar night in the high-Arctic, while summer Hg deposition enhancement has been observed across the tundra due to increased vegetation uptake (Obrist et al., 2017; Zhang et al., 2009). Wet deposition of Hg is defined as the air-to-surface flux in precipitation (occurring as rain, snow, fog or ice) which primarily scavenges GOM and PHg from the atmosphere. Wet deposition of GOM and PHg is estimated to contribute a small proportion of Hg to polar environments, accounting for approximately 5% of all deposited Hg (Obrist et al., 2017).

Mercury deposited to the Arctic surfaces can either undergo photoreduction, and be emitted back to the atmosphere (Kamp et al., 2018), enter aquatic ecosystem, be deposited directly to ocean surfaces, or transferred to long-term terrestrial surfaces. Mercury enters aquatic ecosystems primarily during snow melt and is estimated to deliver between 44 and 50 Mg yr^{-1} (Dastoor and Durnford, 2013; Sonke et al., 2018), while Hg deposited directly to ocean surfaces delivers an estimated 6.5 Mg yr^{-1} (AMAP, 2021). Long-term Hg stores within the Arctic region primarily consist of tundra soils and permafrost, with global stores estimated to be 143 Gg (Obrist et al., 2017). Cycling of Hg is expected to be sensitive to the rapid changes taking place in the region in recent decades (Macdonald et al., 2005; Stern et al., 2012; Schuster et al., 2018; Chetelat et al., 2022). Despite a predicted global decrease in anthropogenic emissions of Hg, an increase in GEM evasion is also predicted due to higher temperatures, permafrost thawing and lower sea ice cover, with further enhancement caused by increased net photochemical GOM reduction within the Arctic substrates which in turn creates a larger surface pool of Hg for evasion (Obrist et al., 2011; O'Driscoll et al., 2006; DiMento et al., 2019).

During spring in polar regions, chemical reactions involving reactive halogens cause the rapid oxidation of GEM to GOM and PHg compounds within the boundary layer to be rapidly deposited to the snowpack during episodes known as atmospheric mercury depletion events (AMDE) (Schroeder et al., 1998; Lu et al., 2001; Ariya et al., 2004; Lindberg et al., 2002; Steffen et al., 2003; Goodsite et al., 2004, 2012; Skov et al., 2006). GEM is photochemically oxidised, mainly by bromine atoms, to inorganic mercury compounds in the gaseous form (GOM) and results in a concurrent depletion of GEM and increase in oxidised mercury species (Wang et al., 2019). AMDE's commonly occur in coastal and marine Arctic environments, initiated by cold temperatures, a stable inversion layer, sunlight, and increased photochemical production of bromine species from the snowpack (Dommergue et al., 2010; Nguyen et al., 2009; Yang et al., 2008, 2020). The presence of sea salt in sea ice, snow and frost flowers provides large sources of these reactive halogen species in the high-Arctic (Moore et al., 2014; Toyota et al., 2014; Wang et al., 2019). Reactive bromine atoms and therefore AMDE's have also been observed in sub-Arctic inland regions, though to a lesser extent (Agnan et al., 2018). A substantial fraction of Hg deposited to snow (up to 90% in some estimates) during AMDE's can undergo rapid photoreduction and re-emission back to the atmosphere (Poulain et al., 2007; Brooks et al., 2006; Steffen et al., 2015). Estimates of the percent of AMDE-sourced Hg remaining in the snowpack a week after deposition range from 5 to 60% with higher retention reported predominantly from coastal locations (Douglas and Blum, 2019).

Global atmospheric Hg trends over the last 10–20 years have not shown spatially or temporally uniform decreases, despite decreasing anthropogenic emissions in most parts of the world. Mace Head, Ireland, the longest background monitoring site has seen a decrease of $-1.69\%\ yr^{-1}$ between 1996 and 2013 (Weigelt et al., 2015), while Cape Point in the Southern Hemisphere has observed a decrease in Hg concentration of $-0.17\%\ yr^{-1}$ between 1994 and 2004, and a switch to increasing Hg of $2.6\%\ yr^{-1}$ from 2007 to 2015 (Martin et al., 2017). Further, anthropogenic emissions are still on the rise despite reductions in North America ($-4.6\%\ yr^{-1}$) and Europe ($-3.5\%\ yr^{-1}$) from 2000 to 2015 (Streets et al., 2019). Global anthropogenic emissions have increased by $1.1\%\ yr^{-1}$ between 2000 and 2015 (Streets et al., 2017). This increase is largely driven by increases across Asia, Central America and east Africa. East Asian emissions have started to decline over recent year but remain the largest emitters (Streets et al., 2019). Arctic atmospheric Hg trends have been estimated to be decreasing at a slower rate that other parts of the world. Previous trend analysis estimated a decrease of $-0.6\%\ yr^{-1}$ from 1995 to 2007 (Cole and Steffen, 2010; Cole et al., 2013). This decrease is largely driven by reduced emissions across North America and Europe. The slower decreasing trend is thought to be influenced by continued high emissions from Asia. The number of air masses arriving at the Arctic originate from Asia is predicted to be

between 30 and 35% (Durnford and Dastoor, 2011). Decreases in sea ice extent causes greater Hg ocean evasion, and is thought to be further slowing atmospheric Hg reductions in the Arctic (Ma et al., 2011; Cole et al., 2013).

As global anthropogenic Hg emissions continue to change, and as the Arctic continues to undergo dynamic and dramatic environmental changes, the continuous monitoring of atmospheric Hg is necessary to provide information about long-term changes in the transport, chemistry, and deposition of atmospheric Hg in the Arctic environment. Expansion of monitoring sites across the Arctic over the last 20 years has led to an increase in spatial and temporal measurements of atmospheric mercury. Comparison of these Arctic sites, collected as part of the Arctic Monitoring and Assessment Programme's (AMAP) 2021 Mercury report, will allow for an extensive evaluation of the observed trends over the past 20 years. This can provide insight not only into trends that may be related to changing emissions, but also into trends that may be due to the influence of other changes that the Arctic is undergoing, including those directly and indirectly associated with climate warming. Increased spatial coverage also allows for a greater understanding of how the differences in atmospheric processes and anthropogenic inputs between the inland and coastal Arctic sites affect seasonal concentrations and trends.

2. Methods

2.1. Site overview

Continuous atmospheric Hg observations were available from 10 long-term Arctic mercury monitoring stations across the circumpolar Arctic region, with temporal coverage varying from 5 years to 23 years (Fig. 1). These include four high-Arctic background air monitoring stations (Alert, Canada; Villum Research Station (Station Nord), Greenland; Zeppelin Mountain Research Station (Ny-Ålesund, Svalbard), Norway and Amderma, Russia), four sub-Arctic sites and two boreal sites above 60° N, listed in Table 1. High-Arctic sites are defined here by their position above 50°N latitude, while sub-Arctic sites are defined by their location between 60°N and 50°N. The two southern Finnish sites of Hyytiälä and Virolahti are located within the northern boreal region, however given their location above 60°N, they are both classified as sub-Arctic in the context of this report.

Continuous measurements presented here are form the start of each sites continuous record to the end of 2018. Mercury air monitoring at Amderma, Russia has been conducted from 2001 to 2009 and between late-2015 and early-2017, but 2015 and 2017 data were not included in the trend analyses due to the data gap between 2009 and 2015. Similarly,

Fig. 1. Map of atmospheric mercury measurement sites for all sites and corresponding measurement years included in this study.

Table 1
Arctic monitoring sites information, including country, location, measurement type, number of measurement years, start and end year.

Country	Location	Measurement	Years (*n*)	First year	Last year
Coastal high-Arctic					
Canada	Alert	TGM	24	1995	Current
		GEM/GOM/PHg	17	2002	Current
Greenland/Denmark	Villum Research Station	TGM (GEM)	11	2008	Current
Norway	Zeppelin (Svalbard)	TGM (GEM)	18	2001	Current
		GOM/PHg	12	2007	Current
Russia	Amderma	TGM	9	2001	2009
Continental sub-Arctic					
Canada	Little Fox Lake	TGM	12	2007	Current
Finland	Hyytiälä	TGM	11	2009	Current
Finland	Pallas	TGM	11	2008	Current
		Manual TGM	23	1996	Current
United States	Denali National Park	TGM	5	2014	Current
Coastal sub-Arctic					
Norway	Andøya	TGM (GEM)	9	2010	Current
Finland	Virolahti	TGM	11	2008	Current

data for Villum for the period of 2001 and mid-2002 were excluded from trend analysis because of the large data gap between these earlier times and the continuous monitoring that started in 2008. TGM has also been collected manually during 24 h periods with a frequency of 1 to 2 samples per week at Pallas since 1996. Two of the coastal high-Arctic sites, Alert and Zeppelin, have long-term GOM and PHg mercury measurements covering the periods 2002-present and 2007-present, respectively. Air monitoring locations are shown in Fig. 1.

2.2. Mercury measurements

2.2.1. Total Gaseous Mercury/Gaseous Elemental Mercury

Mercury measurements at all sites were made using Tekran 2537 (2537a, 2537b and 2537x) automated mercury analyzers that have been described in detail elsewhere (Schroeder et al., 1999). In brief, ambient air was drawn from a 0.2 μm Polytetrafluoroethylene (PTFE) filter through a 50 °C heated sample line by a pump at a flow rate of 1 to 1.5 lpm. Samples are collected at continuous 5 to 15 min intervals via gold trap amalgamation, then thermally desorbed in mercury free air and analyzed using Cold Vapour Atomic Fluorescence Spectrometry (CVAFS). Automated calibration of the analyzer was at a frequency between 23 and 71 h using the internal mercury permeation source, which was verified typically annually. The available air monitoring data is reported as hourly-averaged data; these were aggregated to daily mean concentrations prior to statistical analysis. Data were only considered acceptable for statistical trend analysis when there was 75% daily coverage, to avoid bias caused by diurnal variations.

At Villum, Zeppelin and Andøya a soda-lime trap is installed before the instrument filter and changed at weekly to bi-weekly intervals (Skov et al., 2020; Berg et al., 2013). The trap is primarily intended to prevent passivation of the gold traps. The inclusion of the soda-lime trap is also assumed to remove GOM from the sample line before it can enter the 2537 system (Steffen et al., 2002). Debate still exists surrounding the effectiveness of GOM removal via the use of Teflon filters. Given that only 3 sites employ the soda-lime traps and all sites utilise Teflon inlet filters, there is potential for some GOM to make it through the filters and be measured by the analyzer. Therefore, we have decided to refer to all measurements made using the Tekran 2537 as Total Gaseous Mercury (TGM). As GEM forms such a high proportion of TGM, it is assumed this will have little bearing on the overall trend calculations.

Samples collected with manual traps at Pallas, Finland are collected by pumping a measured volume of air through gold coated quartz trap integrated over a 24 h period and at a frequency of 1 to 2 per week. The traps are then analyzed at the Swedish Environmental Research (IVL) laboratory using CVAFS (Brosset and Iverfeldt, 1989; Iverfeldt, 1991).

2.2.2. Speciated mercury

Speciated mercury measurements at Alert and Zeppelin were collected using Tekran Mercury 1130, 1135 and 2537 speciation unit with an elutriator inlet to remove particulate matter >2.5 μm. GOM samples are operationally defined as mercury which sticks to a KCl coated annular denuder. GOM is measured by pumping sample air through a KCl-coated quartz denuder at a rate of 10 lpm. Sample air then passes through a 0.1 μm quartz particulate filter trap to the 1135 units where PHg is collected. Gaseous Elemental Mercury is not collected in either the particulate filter or the denuder and is sub-sampled from the larger flow by the Tekran 2537 analyzer. GOM and PHg concentrations can be very low and as such air samples collect on the traps for 1 to 2 h. After the collection period, GOM and PHg are sequentially thermally desorbed, pyrolyzed to GEM in zero air and analyzed by the 2537 unit over a 1 h period. Research has suggested that some instrument bias exists where high humidity and ozone can cause a low bias in the measured GOM (Gustin et al., 2013; Lyman et al., 2010; Lyman et al., 2016). However, the conditions under which the experiments from this paper took place are not present in the high-Arctic where humidity is significantly lower and ozone is near zero during the elevated GOM/PHg collection period. There is currently no evidence to suggest that high-Arctic conditions show any effect on denuder performance. Reported data for the GOM and PHg monitoring programs at Alert and Zeppelin varied (between 2 and 3 h intervals) and there was a slight difference between the two data sets in the way GOM and PHg concentrations were calculated in the reported data. Due to the high GOM concentrations from springtime AMDE's, high values can be observed in the flush cycles and are not included in the zero subtraction from GOM and PHg in the RDMQ process (Steffen et al., 2013). Therefore, concentrations from Alert were recalculated from the raw data to match the zero subtraction method used in Zeppelin data. GOM and PHg daily mean concentrations were accepted for trend analyses if they met the 75% daily maximum coverage requirement to account for diurnal variability.

2.3. Mann-Kendall trend analysis

Due to the large size of the individual datasets, continuous measurements for both TGM and speciated Hg were first averaged at daily intervals prior to any further analysis. Therefore, all concentrations are reported as daily mean concentrations. All further statistical and trend analysis was then preformed using these daily mean concentrations. Trend analysis was preformed using the Mann-Kendall test for trend and the related Sen's slope calculation analysis (Gilbert, 1987). Trends were calculated for annual and seasonal changes in TGM concentrations using daily mean Hg data, and for annual and monthly changes in GOM and PHg concentrations at Alert and Zeppelin. The Mann-Kendall test determines the presence of a trend by first separating each season (or month) into its own dataset, each daily mean TGM (or GOM, or PHg) value within the separated dataset is then treated as a replicate value. The trend is confirmed or rejected by the Mann-Kendall test. Slopes are then determined using Sen's nonparametric estimator of slope (Cole and Steffen, 2010; Cole et al., 2013). This method has been used to assess temporal trends with atmospheric mercury data sets such as those from the Arctic, sub-Arctic and temperate sites (Berg et al., 2013; Cole and Steffen, 2010; Cole et al., 2013; Gay et al., 2013; Weiss-Penzias et al., 2016). The extension of the non-parametric Mann-Kendall method is recommended for use on data that is not normally distributed, and which may have data gaps; both these conditions are present in these datasets.

Data is presented here as the median change in TGM concentrations (in ng m^{-3}) as a percentage of that sites season's mean concentration. Trends were considered statistically significant from zero only if the upper and lower 95% confidence intervals of the Sen slope were either both above zero or both below zero. A significant positive trend is indicated if both the median trend and the 95% confidence intervals are above the

zero line, while a significant negative trend is indicated when median trend and 95% confidence interval is below zero. Data analyses were performed for both entire time series at each site and for overlapping time series from the decadal period 2008–2018. This dual approach permits the best understanding of trends at individual sites, as well as a direct comparison of trends over a consistent period between sites. Alert and Zeppelin's continuous GOM and PHg trends were determined in the same way, except trends were separated into monthly bins rather than the seasonal trend of TGM. This finer resolution was done to better capture the high variability of PHg and GOM during both spring and summer.

3. Results and discussion

3.1. Seasonality of atmospheric mercury

The behaviour of annual and seasonal TGM concentrations were examined to ascertain both inter-site and intra-site variability. Daily mean TGM concentrations were split between four seasons: winter (December, January, February); spring (March, April, May); summer (June, July, August) and fall (September, October, November). Broadly, seasonal patterns of TGM concentration were observed to be different in the high-Arctic compared the sub-Arctic (Supplementary Table 1). The highest annual mean concentration for high-Arctic coastal sites (Alert, Amderma, Zeppelin and Villum) was at Amderma, 1.5 ng m^{-3} (SD 0.3 ng m^{-3}), while the lowest was Villum 1.3 ng m^{-3} (SD 0.4 ng m^{-3}). The high TGM concentrations at Amderma are likely because measurements were only available from 2001 to 2009, while all other Arctic sites indicate that decreasing TGM concentrations started to occur after 2010 (Fig. 2). High-Arctic sites also showed the largest annual range and standard deviation of daily mean TGM concentrations (Supplementary Table 1). The lowest annual mean concentrations for the sub-Arctic sites were observed at Hyytiälä 1.2 ng m^{-3} (SD 0.2 ng m^{-3}), while highest annual mean concentrations were at Andøya 1.5 ng m^{-3} (SD 0.2 ng m^{-3}).

High-Arctic sites have been reported to experience large variability during summer and spring caused by the different deposition processes associated with AMDE's (Berg et al., 2013; Steffen et al., 2014, 2015; Skov et al., 2020; Fisher et al., 2012). AMDE's are the conversion of stable GEM to rapidly depositing GOM and PHg and will result in periods of low GEM air concentrations. Periods of elevated GEM or TGM have also been reported during these periods and were attributed to rapid reduction of deposited GOM to GEM and emission from the surface (AMAP, 2011; Steffen et al., 2013). At the high-Arctic sites measured here, lowest seasonal mean TGM concentrations were observed during spring. However, spring was also observed to have the highest daily TGM mean concentrations, Alert (3.3 ng m^{-3}), Amderma (4.2 ng m^{-3}) and Villum (2.9 ng m^{-3}). The only exception was Zeppelin which saw its highest daily mean in summer of 2.4 ng m^{-3}, compared to spring with a highest daily mean of 2.4 ng m^{-3}. Spring also exhibited the largest TGM variability with standard deviations ranging from 0.3 ng m^{-3} at Zeppelin to 0.6 ng m^{-3} at Villum.

Summer recorded the highest seasonal mean TGM concentrations and variability at the high-Arctic Zeppelin, Alert and Villum (with the exception of Amderma where winter had the highest concentration). The summer enhancement is still not fully reconciled, but is thought to result from a combination of re-emission of AMDE deposited mercury, other emissions of mercury from surfaces (e.g., tundra, lakes etc.), snow melt and evasion from the Arctic Ocean fed by Arctic rivers (Steffen et al., 2005; Fisher et al., 2013; Angot et al., 2016; Sonke et al., 2018). The duration and magnitude of AMDE's change year to year due to meteorological conditions and this impacts inter-annual variability of the seasonal concentrations as shown in Fig. 2 (Steffen et al., 2008). Villium had the highest spring and summer inter-annual range, 1.4 ng m^{-3} and 0.9 ng m^{-3} respectively, which shows greater inter-annual variability during spring and summer at high Arctic sites (in blues) than during winter and fall. Changes in the spring and summer concentrations may therefore indicate changes to either mercury inputs (global or regional) or localized chemistry that affects concentrations.

Seasonality at the sub-Arctic sites varied between locations. In general, highest daily mean maximum TGM concentrations were observed during the winter and/or spring period. Winter maximums were observed at the coastal sites Andøya, (1.6 ng m^{-3}), Virolahti (1.4 ng m^{-3}) and the inland site of Pallas (1.5 ng m^{-3}). Spring seasonal daily mean maximums were observed for Denali National Park (1.4 ng m^{-3}), Little Fox Lake (1. 5 ng m^{-3}), and Hyytiälä (1.3 ng m^{-3}), all of which were inland sites. Mean seasonal concentrations for the inland sites were observed to be the lowest during the fall season for Hyytiälä (1.1 ng m^{-3}), Virolahti (1.2 ng m^{-3}), Denali National Park (1.2 ng m^{-3}), Pallas (active sampling: 1.3 ng m^{-3} and manual sampling: 1.3 ng m^{-3}) and Little Fox Lake (1.3 ng m^{-3}) (Supplementary Table 1). Inland Arctic sites have been observed to have lower TGM

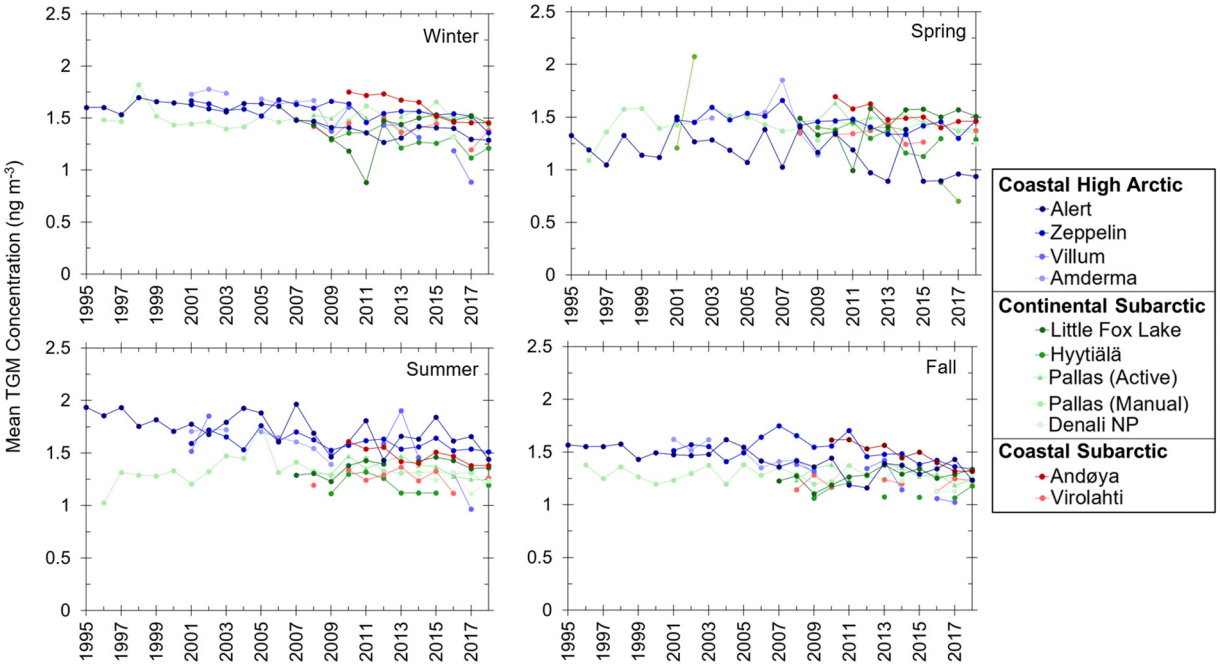

Fig. 2. Seasonal mean TGM concentrations in air (ng m^{-3}) for each measurement year at 10 circumpolar locations.

concentrations during spring as there is an increased uptake of Hg by vegetation during the growing season, resulting in reduced seasonality (Obrist et al., 2017; Chetelat et al., 2022). Jiskra et al. (2018), observed that at sub-Arctic sites (and throughout the northern hemisphere) lower concentrations of TGM are typically observed during the summer and fall, with minima typically observed in September. These annual atmospheric mercury patterns in the northern hemisphere are thought to be the result of the respiration process incorporating GEM into plant tissue during the growing season (Jiskra et al., 2019; Obrist et al., 2017).

Clear differences in TGM concentrations were observed between coastal and inland sub-Arctic sites. The coastal sites Andøya and the inland site, Pallas, are located at similar latitudes, approximately 350 km inland from the coast. Annual mean daily mean TGM concentrations were lower for the inland Pallas site (1.4 ng m^{-3}, SD 0.1) than the coastal Andøya (1.5 ng m^{-3}, SD 0.1). A lower concentration and less variability (lower standard deviation, Supplementary Table 1) at the inland Pallas site were also observed for each season. Similarly, the coastal site Virolahti is at approximately the same latitude to Hyytiälä which is located 230 km inland. Lower annual mean concentrations were observed at the inland site Hyytiälä (1.2 ng m^{-3}, SD 0.2) compared to the similar coastal site Virolahti (1.3 ng m^{-3}, SD 0.2). Differences between coastal and inland Artic sites have been observed, although these are largely dependent on plant productivity, with more northern sites having shorter growing seasons (Olson et al., 2019). Both Hyytiälä and Virolahti are located in boreal regions where net primary productivity (NPP) is higher (Li et al., 2017) and exhibited lower TGM concentrations compared to Pallas and Andøya located further north where mean TGM concentrations were lower. NPP have also been shown to decrease with higher latitudes (Li et al., 2017). Obrist et al. (2017), observed that dry deposition driven by the presence of vegetation in the tundra was the dominate source of Hg (71%; 6.5 μg m^{-2} yr^{-1}) to the region. Changes in vegetation growth patterns in the Arctic caused by climate change may influence the uptake of mercury during short growing seasons (Agnan et al., 2018; Chetelat et al., 2022).

3.2. Temporal trends in Total Gaseous Mercury (TGM)

Seasonal and annual temporal trends using daily mean TGM concentrations were calculated for each site. Data coverage varied between the sites, complicating trend analysis interpretation. Seasonal trend analyses were performed using all available data collected from each site (Fig. 3) and are presented as the median change in TGM as a percentage. Annual median TGM trends for all available years were negative for 8 of the 11 measurements. Largest annual changes occurred at Villum −2.81% yr^{-1} and Amderma −2.28% yr^{-1}. Zeppelin and Alert experienced the least significant negative change over their entire record, −0.57% yr^{-1} and −0.95% yr^{-1}, respectively (Fig. 3, Supplementary Table S2). Virolahti and Pallas (manual sampling, 1996–2018) show no significant annual trend, while Little Fox Lake was the only site to have a significant positive (increasing) annual trend (Fig. 3). Manual sampling at Pallas introduces a higher amount of error due to the lower frequency of collection (one or two 24 h samples per week) and higher measurement uncertainty, which likely causes the smaller trend compared to the continuous sampling trend, which is also reported for a different time period. Trends across all seasons were negative at the majority of sites with the exception of Little Fox Lake (all seasons, significant), Hyytiälä (fall, but not significant), Virolahti (summer, not significant, and fall, significant) and Denali National Park (fall, but not significant, Fig. 3). Of the sites that had significant negative trends (Pallas, Amderma, Zeppelin, Alert, Villium and Andøya), Villum had the largest significant winter trend (−4.55% yr^{-1}), while smallest significant trend was at Zeppelin during fall (−0.76% yr^{-1}). Sea ice cover around Villum Research Station, Greenland has changed dramatically over the last decade, becoming more seasonal, and therefore changing deposition patterns and leading to the large reduction in TGM concentrations (Selyuzhenok et al., 2020). Fall is considered the best period to examine the northern hemispheres TGM background concentrations in the high-Arctic, as it is not influenced by processes that increase seasonal variability (e.g. AMDEs) (Jiskra et al., 2018; Skov et al., 2020). The negative fall trend at Zeppelin indicates that decreases in the Northern Hemisphere global background concentration are also observable in the high-Arctic.

In order to provide a direct comparison of trends between sites with different length data records, Mann-Kendall seasonal and annual trend analysis was also preformed for the years 2008–2018, the period for which there was the most concurrent data collected (Fig. 4). Hyytiälä data record started in 2009, while Andøya measurement commenced in 2010. Denali National Park only has data coverage for 5 years so its interpretation remains limited and Amderma was not included as data coverage was not sufficient for this period. The overall annual TGM trends of the overlapping 2008–2018 period are similar to the trends calculated for all the years of data. Annual significant negative trends ranged from −0.87% yr^{-1} at Pallas (active) to −4.15% yr^{-1} at Villum. Both Virolahti and Pallas (Manual) had no

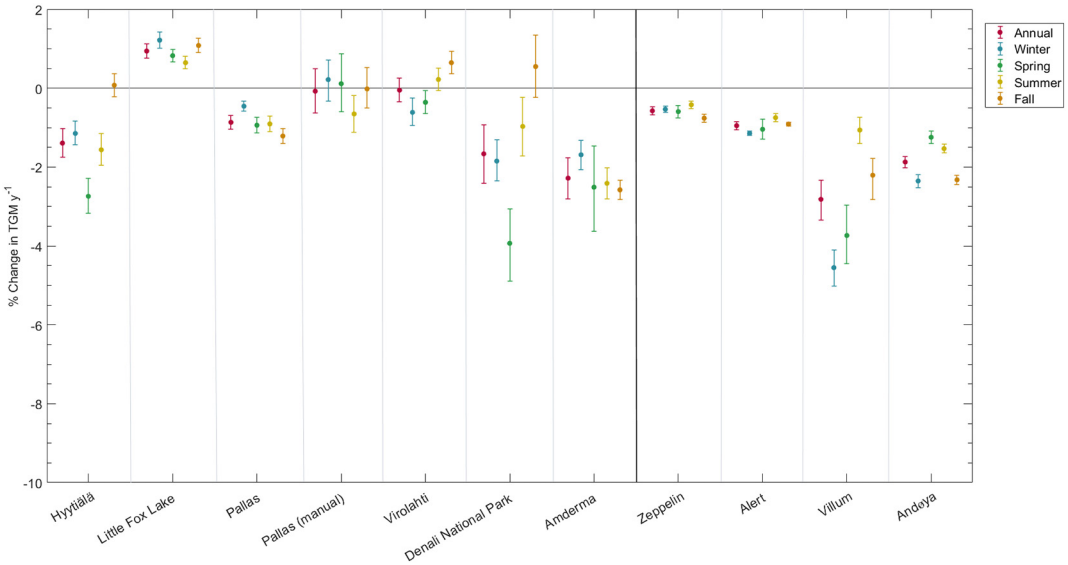

Fig. 3. Seasonal and annual median trends (red), winter (December to February, blue), spring (March to May, green), summer (June to August, yellow), fall (September to November, orange) respectively, in TGM based on daily mean concentrations for all sites across all reported years. The error bars show upper and lower 95% confidence intervals. If the error bars are below the grey zero line it indicates a decreasing trend and if they are above the zero line it indicates an increasing trend. If the zero line on the y-axis falls within the bars, no significant trend is reported.

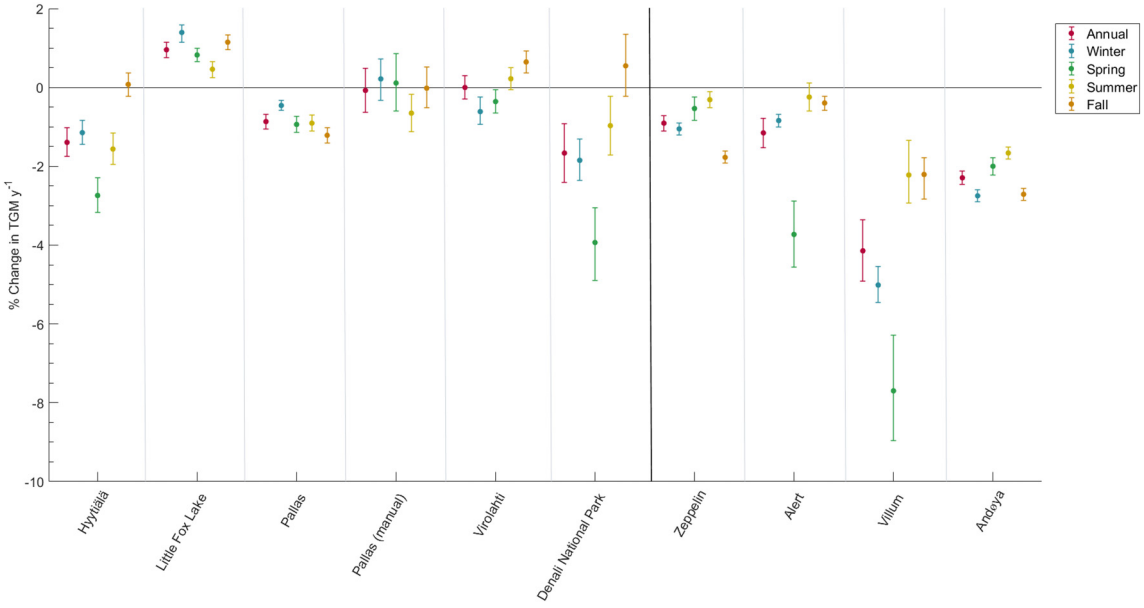

Fig. 4. Seasonal and annual median trends (winter, spring, summer, and fall respectively by site) in TGM based on daily mean concentrations measured at each site 2008–2018. The error bars show upper and lower 95% confidence intervals. If the error bars are below the grey zero line it indicates a decreasing trend and if they are above the zero line it indicates an increasing trend.

significant trend and Little Fox Lake was the only site with a positive trend (0.96% y^{-1}). In general, seasonal trends for 2008–2018 showed larger decreases than observed for all year trends. Across the high-Arctic sites, Alert and Villum experienced largest significant decline in spring, $-3.73\%\ yr^{-1}$ and $-7.70\%\ yr^{-1}$ respectively, while Zeppelin saw greatest decline in in Fall ($-1.77\%\ yr^{-1}$) (Fig. 4). Smallest decreases occurred in summer for all high-Arctic sites. This is mostly likely driven by the enhanced surface emissions in the high-Arctic during summer (Steffen et al., 2005; Cole et al., 2013).

The sub-Arctic sites fall trends were not significant for all sites, except Andøya and Pallas (Active, significant negative trends) and Little Fox Lake which had a significant positive trend ($1.38\%\ yr^{-1}$). Spring trends across all sites had the greatest statistically significant negative changes ranging between $-7.70\%\ y^{-1}$ at Villum and $-0.36\%\ y^{-1}$ at Virolahti and all sites had significant negative trends, with the exception of Pallas (Manual) and Little Fox Lake. This may indicate that more Hg uptake is occurring as a result of increasing plant uptake. Warmer temperatures and reduced snow cover are changing the Arctic growing season, with active layer freezing occurring later in the year and increased greening across the Arctic (Lund, 2018), which may cause further decreases to the atmospheric TGM during this time (Chetelat et al., 2022).

The annual concentration at Little Fox Lake is increasing by $1.00\%\ yr^{-1}$ per year for the 2008–2018 period. More so, the winter concentrations, when the atmospheric TGM is not subject to vegetative uptake show an even larger positive trend at $1.39\%\ yr^{-1}$. This represents the only positive annual and winter trend in the Arctic. The under-lying driver of this increasing trend is not fully understood. One possible explanation is an increase in the relative frequency of air masses arriving at Little Fox Lake from Asia (Huang et al., 2017), coupled with increased Hg emissions from the region. Another is the frequent occurrence of wild fires along the west coast of Canada leading to enhanced Hg emissions (Fraser et al., 2018).

Comparing the 2008–2018 trends to the all year trends, for those sites that have longer available datasets, we are able to determine how these trends have changed over the recent decade. For example, Alert's spring trend was $-1.04\%\ yr^{-1}$ across the entire record, compared to a decrease of $-3.73\%\ yr^{-1}$ between 2008 and 2018 periods, which represents an increase in the rate of decline during the latter period. Similarly, the negative trend for the Zeppelin fall period increased from $-0.76\%\ yr^{-1}$ between 2001 and 2018 to $-1.77\%\ yr^{-1}$ between 2008 and 2018. Both Alert and Zeppelin show an accelerated decreasing trend than previously reported (Cole et al., 2013; Berg et al., 2013). Cole and Steffen (2010), found that Alert TGM concentrations was decreasing at a rate of $-0.56\%\ yr^{-1}$ from 1995 to 2007, while Zeppelin showed no significant trend between 2000 and 2009 (Berg et al., 2013) and a small negative but not significant trend was observed between 2009 and 2014 (Skov et al., 2020). The changing trends at the two high-Arctic sites of Alert and Zeppelins suggests that changes in global emissions and concentrations are only recently observable in the Arctic and further demonstrate that the trends themselves at an individual site can and are changing over time.

In order to examine more closely how these TGM trends have changed over the measurement periods, 5 year moving trends were calculated for Alert, Zeppelin and Pallas (active) (Fig. 5). Mann-Kendall TGM trends are calculated over a 5 year period, the recommended minimum time series to satisfy Mann-Kendall statistical conditions, starting from the first years measurements then shifted up one year and calculated for the preceding 5 years. This allows for a more detailed exploration of how the trends have been changing over time. The shifting trend analysis was preformed for the longest running sites of Alert (1995–2018), Zeppelin (2001–2018) and for Pallas (active, 2008–2018), which was the longest running sub-Arctic site with significant trends across all seasons (Fig. 5). Alert 5-year shifting trends show more variability than the other two sites, particularly during spring and summer (Fig. 5a). This most likely reflects the high variability in the timing and strength of AMDEs that typically occur during this time. Alert's summer trends have the smallest variability, ranging from -0.08 to $0.06\%\ yr^{-1}$. This may be a reflection of elevated local TGM emission that commonly occur in summer, such as enhanced ocean invasion or emission from melting ice and snow (Steffen et al., 2008). Fall trends show a positive trend from 2001 to 2008, trends then sharply decrease before becoming steady from 2011 to 2018. Pallas' (active) 5-year trends from active monitoring appear to be reasonably uniform between seasons (Fig. 5c). All seasons show an accelerated declining trend from 2008 to 2012, switching from a positive trend to a negative trend. Trends seem more consistent in the later part of the decade (2012–2018). Zeppelin tends to show a similar overall variability in trends as Alert does, although appears to have a more consisted declining trend.

3.3. Trends in speciated mercury at Alert and Zeppelin

Alert and Zeppelin are the only 2 sites that have available long term continuous speciated mercury data including GOM and PHg. Daily mean

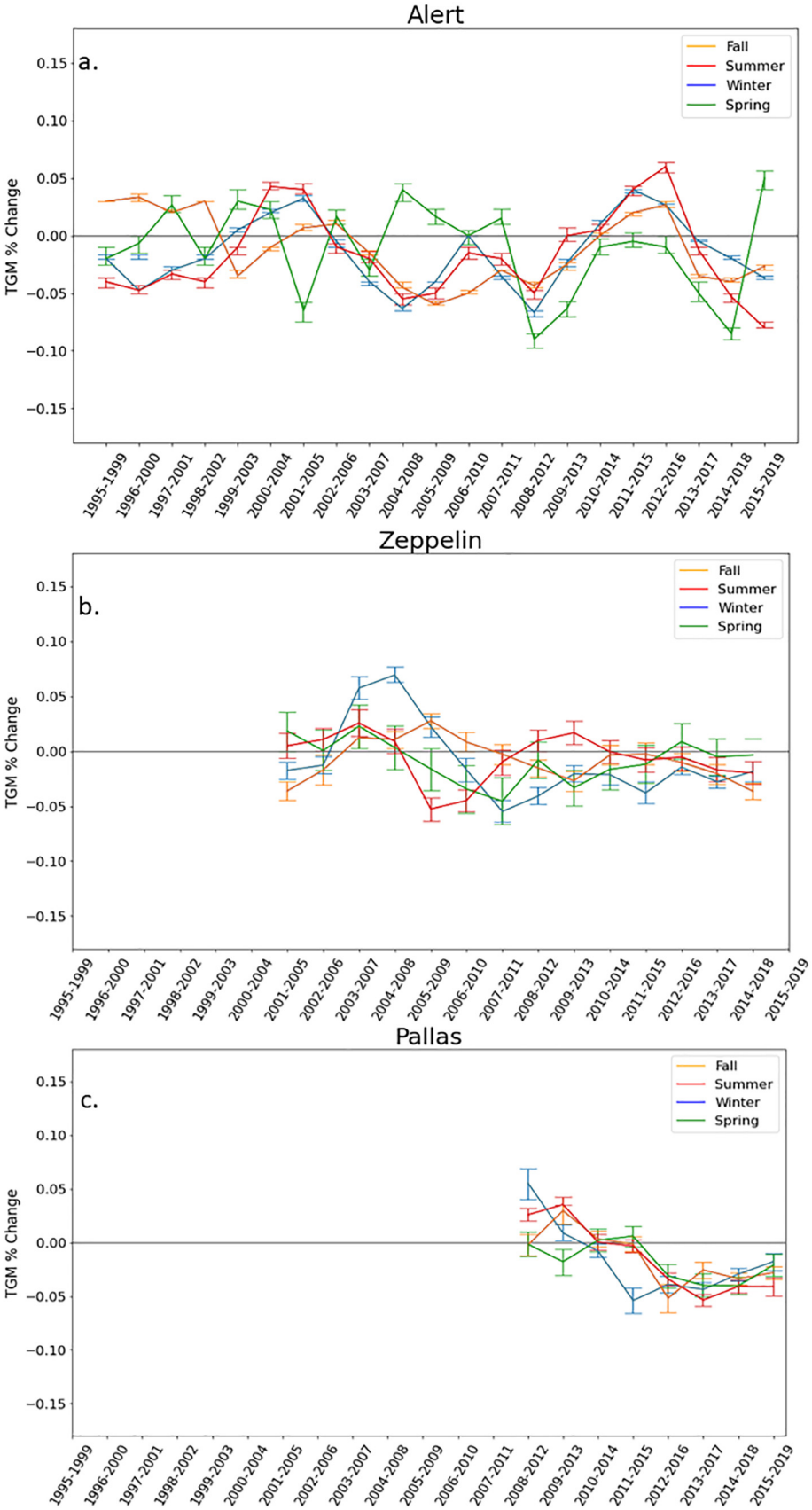

Fig. 5. Five-year shifting trend vales at Alert (a, 1995–2018), Zeppelin (b, 2001–2018) and Pallas Active (c, 2008–2018). Solid line show median seasonal trends (Fall; blue, Summer; red, Winter; yellow, Spring; green) determined at 5 year values. Error bar represent the 95% confidence intervals.

concentrations of GOM and PHg were calculated from 2002 to 2018 at Alert and from 2008 to 2018 at Zeppelin. These high-Arctic sites are known to have significant seasonal variability in GOM and PHg concentrations (Steffen et al., 2008), which would otherwise be lost in the courser seasonal trend analysis used for TGM measurements (Fig. 6). In order to fully capture this variability monthly trends were examined for these 2 datasets rather than the seasonal trends used for the TGM datasets. Annual mean GOM and PHg concentrations at Alert was 24 pg m^{-3} (SD 41 pg m^{-3}) and 38 pg m^{-3} (SD 52 ng m^{-3}), respectively (Supplementary Table 3). Monthly mean concentrations peaked in May for GOM and April for PHg (Fig. 6). Alert's high PHg concentrations, particularly during spring, are thought to be enhanced by GOM preferentially adhering to increased particles present in the atmosphere that result from processes such as Arctic haze (Steffen et al., 2014). Zeppelin annual concentrations were 18 pg m^{-3} (SD 8 pg m^{-3}) for GOM and 5 pg m^{-3} (SD 3 pg m^{-3}) for PHg. Concentrations of GOM and PHg both peaked in April, coinciding with the timing of AMDEs for the region. These speciation concentrations for both Alert and Zeppelin are notably higher than those measured outside the Arctic with median GOM concentration found to range between 1 and 3 pg m^{-3} and PHg concentrations range between 3 and 5 pg m^{-3} across all AMNet sites (Gay et al., 2013).

Similar to the TGM trend analysis, speciated Hg trend analysis was preformed for the entire sampling period at Alert (2002–2018) and Zeppelin (2008–2018) and for the overlapping years (2008–2018) at Alert for direct comparison. Alert PHg trends for 2002–2018 during the months of January, March, April, June, September, and November were not significant (Fig. 7). The months of February, March, May, July, August, October, and December were observed to have small but significant negative trends of PHg ranging from −0.90% (March) to −7.45% (July). June was the only month to see an increase of 1.52% y^{-1}. Alert GOM concentration trends are fairly consistent across the year for the 2002–2018 period, with all months except February and June having significant positive trends. Alert increase of GOM were largest in January (6.12% y^{-1}) and April (6.90% y^{-1}). The only negative trend was found in February (−1.74% yr^{-1}). June's trend was positive but not significant. Cole et al. (2013) found annually from 2002 to 2009 no significant annual trends for either GOM or PHg but, noted that GOM increased significantly in March, May and July and PHg increased in March, April and July, ranging between 9 and 17% y^{-1}. By comparison the extended trends (2002–2018) calculated here show lower but consistent monthly trends across the whole year.

Comparison of Alert speciation trends for the entire measurement record (2002–2018) with the 2008–2018 trend calculations indicate that there has been a shift in Hg species composition. PHg shows significant monthly trends between 2008 and 2018 range from −3.02% yr^{-1} to −9.11% yr^{-1} (Supplementary Table S4), greater than the 2002–2018 PHg trends. January, March and June switched from no significant trend for all data to a significant negative trend for 2008–2018 (Fig. 7). GOM monthly trends for 2008–2018 varied, such that negative trends are reported in February, July, August, and December while positive trends are reported for January, April and June and no significant trend for all other months. Monthly trend at both Alert and Zeppelin suggest that the composition and timing of AMDEs are changing in the high Arctic. Negative PHg trends at Alert in February increased from −5.85% yr^{-1} (2002–2018) to −9.11% yr^{-1} from 2008 to 2018 (Supplementary Table S4). March PHg trends switched from a not significant trend for 2002 to 2018 to a significant negative trend of −4.79% yr^{-1}, 2008–2018. GOM trends also show a greater negative trend in February, increasing from −1.75 yr^{-1}, 2002–2018, to −3.16% yr^{-1}, while March GOM trends switched from a positive trend of 3.32% yr^{-1} to a not significant trend. The high variability of both GOM and PHg during spring and summer, caused by the occurrence of AMDEs, means that changing trends observed during this time have a greater influence on Alerts overall atmospheric Hg composition than if these changes were to occur at any other time of the year.

Comparison of speciation trends with seasonal TGM trends at Alert indicates that AMDEs have altered. Cole et al. (2013), noted that PHg trends at Alert for 2002–2009, increased during March and April. Trends determined here for 2008–2018 show PHg trends from March to May either decrease or are not significant, while GOM increases in April and is not significant March and May. While Cole et al. (2013) found that GOM increased in May but was not significant March and April for 2002 to 2009. This suggests that while TGM spring concentrations are decreasing, the strength and frequency of AMDE's are not changing. Alerts summer TGM (2008 to 2018) trends show no significant change, however GOM increases in June and then switches to negative trend in July and August, suggesting AMDE's are occurring earlier. Warmer spring temperatures and increased humidity are likely starting to limit the gas-particle separation of GOM to PHg, combined with changing Arctic and sea-salt aerosol dynamics that occur within the Arctic Haze and allow for the oxidation of GEM to PHg (Steffen et al., 2014, 2015; Zheng et al., 2021). Overall, this suggests the AMDEs are occurring earlier in the season and are becoming dominated by GOM deposition.

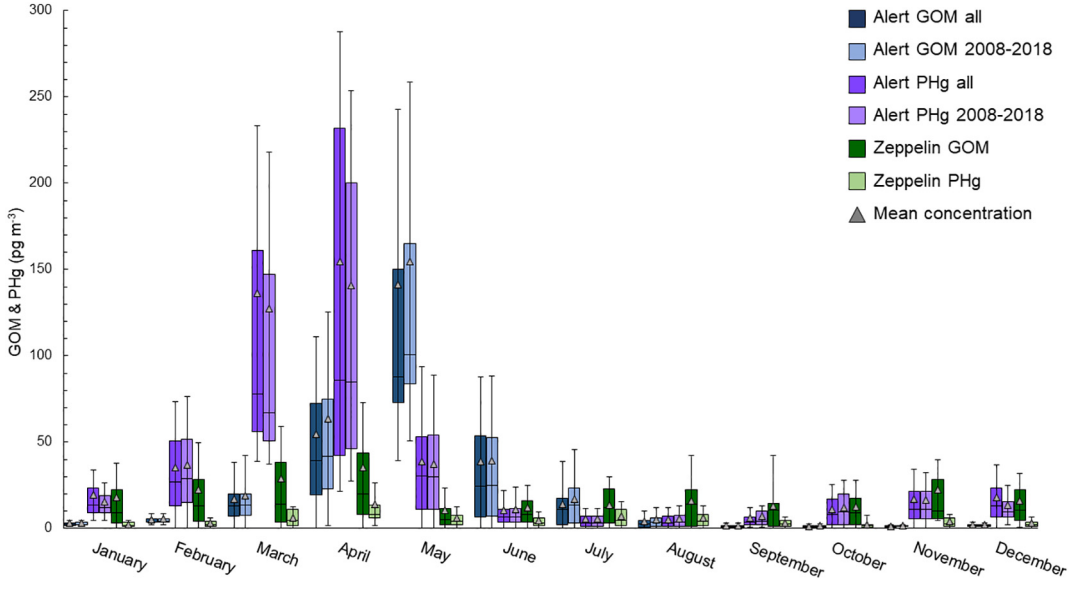

Fig. 6. Monthly summary statistics for Alert and Zeppelin's speciation data. Boxes represent 25% and 75% quartiles, middle line is the median and error bars are the standard deviation of the mean. Grey triangle represents mean concentrations.

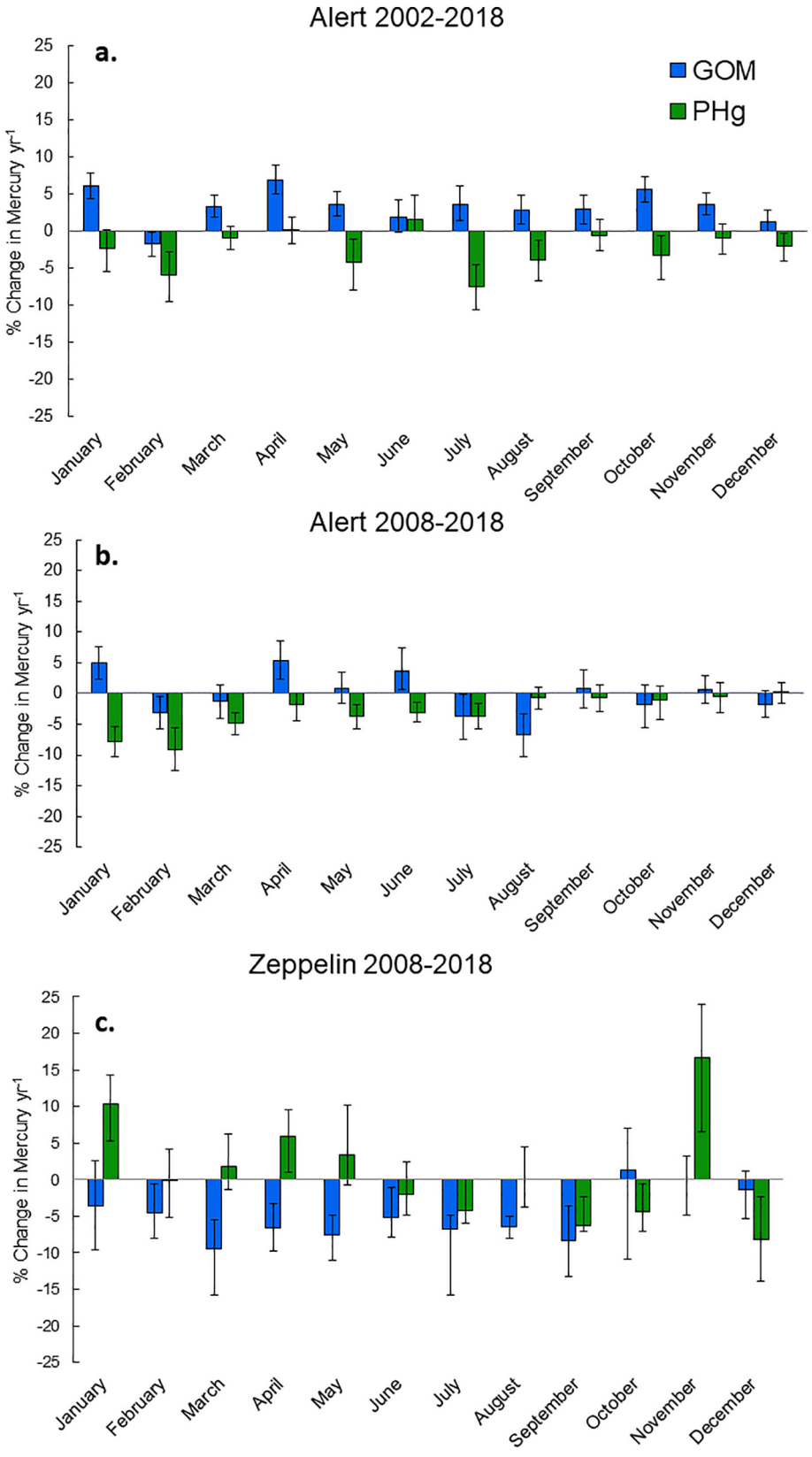

Fig. 7. GOM (blue) and PHg (green) monthly median trends for Alert (2002–2018 and 2008–2018) and Zeppelin (2008–2018) as a change in concentration as a percentage of the monthly mean.

In contrast, Zeppelin (2008–2018) generally saw opposite trends to those observed at Alert. GOM trends at Zeppelin were negative for the months of February through September, ranging between $-8.37\%\ y^{-1}$ to $-4.60\%\ y^{-1}$, with no significant trends for October through to January. Zeppelin's PHg trends were positive for the months of January (10.27% yr^{-1}), April (5.91% yr^{-1}) and November (16.74% yr^{-1}) and negative for

September ($-6.30\%\ yr^{-1}$), October ($-4.33\%\ yr^{-1}$), and December ($-8.16\%\ yr^{-1}$) (Fig. 6). Overall, annual median trends at Zeppelin shows a significant negative GOM trend ($-1.77\%\ yr^{-1}$) and a not significant positive PHg trend, whereas Alert shows a significant negative PHg trend of $-0.93\%\ yr^{-1}$ for 2008–2018 and a not significant positive GOM trend (Supplementary Table S3).

The negative trend in GOM at Zeppelin during spring indicates a change in the conditions under which AMDE's occur at this site, while the positive trend of PHg in April may indicate a higher availability of particulates during this period. Heslin-Rees et al. (2020) found that the rate of coarse-mode particles arriving at Zeppelin has increased by 2.6% to 2.9% between 1999 and 2017. The increase in coarse particle size was attributed to Arctic air masses spending more time over open water and therefore increasing the amount of sea-salt aerosols being transported to the region. Zeppelin AMDE's were assumed to occur via long range transport of GEM depleted air masses over the Arctic Ocean (Gauchard et al., 2005; Steen et al., 2011).

Increasing PHg trends during spring could indicate a change or increase in the amount of long-range transport arriving at Zeppelin (Zhang et al., 2009; Steen et al., 2011). Hirdman et al. (2010) found that the majority of air masses arriving at Zeppelin were transported through Eurasia. Zeppelin AMDE's are the result of long rang transport of GEM depleted air masses arriving at the site. AMDE's in the region typically occur over the Arctic Ocean and then are transported to Zeppelin, where the deposition then occurs. Due to the high deposition velocity of GOM, deposition often occurs before the air masses reach Zeppelin, leading to lower GOM concentrations compared to the PHg (Berg et al., 2013; Steen et al., 2011). Increasing PHg trends could indicate that the frequency of these air masses arriving at this site is increasing over recent years. A review of global sources of Hg emissions and transport to the Arctic, and influences of changes in emissions and meteorology on atmospheric Hg are presented separately in this special issue (Dastoor et al., this issue). Increased first year sea ice and an overall reduced sea ice coverage due to warmer water in the Barents Sea could be further influencing the location, strength and composition of AMDEs occurring near Zeppelin (Steen et al., 2011). Despite the differences in direction, with Alert moving towards positive GOM trends and Zeppelin moving towards positive PHg trends, both sites are showing changes in the process that may affect the deposition and input of mercury to the Arctic environment.

4. Conclusion

The number of Arctic Hg monitoring sites has increased over the last 20 years, which has allowed for a more comprehensive and holistic assessment of how atmospheric Hg patterns are changing across the Arctic. Atmospheric mercury concentrations have been found to be decreasing across much of the Arctic though not uniformly. Sub-Arctic sites generally show the greatest decreases. Seasonal TGM concentrations at the four coastal high-Arctic sites had greater variability than sub-Arctic sites, differences that are driven by local chemistry. Spring saw the greatest decrease, while fall saw the least with most sites not having a significant trend. High-Arctic sites in general saw the smallest annual change. Comparison of the entire data sets with 2008–2018 trends show that for most sites the observable decreases in TGM concentrations have accelerated over the last decade.

Speciation trends at Alert and Zeppelin saw no significant annual trends. Indicating the concentrations overall are remaining the same. However, monthly trends are telling a different story. Alert saw a decrease in PHg concentrations at the start of the year, while GOM trends tended to decrease, suggesting that the gas-particle partitioning that was typically observed to occur at Alert is occurring earlier. Zeppelin saw the opposite occurring with increased PHg and decrease GOM. This indicates that there has been an increase in the amount of particulates present in the Zeppelin providing an increase PHg. The small decrease in TGM during spring and summer coupled with the speciation trends at both Alert and Zeppelin indicate that the occurrence of AMDEs are not decreasing in the high-Arctic but rather the timing and composition of the depletion events is being altered.

Increased monitoring sites across the Arctic have provided a more detailed spatial understanding of changing mercury trends. However, large gaps are still present particularly across Russian and North American Arctic regions. As observed here trends throughout the Arctic are not uniform and filling these gaps would help provide a more holistic understanding of mercury's behaviour throughout these unique environments. Deployment of new monitoring technology, such as passive air samplers could further help bridge these gaps by providing data for regions with limited accessibility or power supple. Understanding of how vegetation in the Arctic influences the deposition and long term storage of mercury is still limited and even less is known about how changing vegetation in the Arctic will influence atmospheric mercury in the future.

CRediT authorship contribution statement

Katrina MacSween: Writing – original draft, Conceptualization, Visualization. **Geoff Stupple:** Writing – review & editing, Conceptualization, Methodology, Validation, Data curation, Investigation, Formal analysis, Visualization. **Wenche Aas:** Writing – review & editing, Methodology, Data curation, Investigation. **Katriina Kyllönen:** Writing – review & editing, Methodology, Data curation, Investigation. **Katrine Aspmo Pfaffhuber:** Writing – review & editing, Methodology, Validation, Data curation, Investigation. **Henrik Skov:** Writing – review & editing, Methodology, Validation, Data curation. **Alexandra Steffen:** Writing – review & editing, Conceptualization, Supervision. **Torunn Berg:** Methodology, Data curation, Investigation. **Michelle Nerentorp Mastromonaco:** Writing – review & editing, Methodology, Data curation, Investigation.

Declaration of competing interest

The authors declare that they have no known competing financial interests or personal relationships that could have appeared to influence the work reported in this paper.

Acknowledgements

ECCC authors acknowledge the team at Dr. Neil Trivett Global Atmosphere Watch Observatory at Alert and Laberge Environmental at Little Fox Lake for the excellent technical work. We also thank Bernard Firanski and Quinn Coughlin for their assistance with the statistical and trend analysis. We thank the Northern Contaminants Program for continued financial support for monitoring programs in Alert and Little Fox Lake. Henrik Skov acknowledges The Danish Environmental Protection Agency (DANCEA funds for Environmental Support to the Arctic Region project; grant no. 2019-7975) and the European ERA-PLANET projects; iGOSP and iCUPE (consortium agreement no. 689443 for both projects) for financial support. The Royal Danish Air Force is acknowledged for providing free transport of the equipment to Station Nord, and the staff at Station Nord are especially acknowledged for their excellent technical support. The Villum Foundation is gratefully acknowledged for financing the new research station; Villum Research Station. Katrine A Pfaffhuber acknowledges the Norwegian Environment Agency for financial support to sustain measurements. KAP is grateful for the technical and logistical support offered by the staff at the Norwegian Polar Institute at the Sverdrup station in Ny-Ålesund, in addition to local site managers at Birkenes and Andøya. Last but not least NILU's excellent technicians and instrument care takers Jan H. Wasseng and Are Backlund are acknowledged. All the co-authors would like to thanks AMAP for the guidance and continuous support for these important monitoring programs. We would also like to thank the National Atmospheric Deposition Program for providing Denali National Park data.

Appendix A. Supplementary data

Supplementary data to this article can be found online at https://doi.org/10.1016/j.scitotenv.2022.155802.

References

Agnan, Y., Douglas, T.A., Helmig, D., Hueber, J., Obrist, D., 2018. Mercury in the Arctic tundra snowpack: temporal and spatial concentration patterns and trace gas exchanges. Cryosphere 12, 1939–1956.

AMAP, 2011. Arctic Pollution 2011. Arctic Monitoring and Assessment Programme (AMAP), Oslo.

AMAP, 2021. 2021 AMAP Mercury Assessment. Summary for Policy-makers. Arctic Monitoring and Assessment Programme, Tromsø, Norway.

Angot, H., Dastoor, A., De Simone, F., Gårdfeldt, K., Gencarelli, C.N., Hedgecock, I.M., Langer, S., Magand, O., Mastromonaco, M.N., Nordstrøm, C., Pfaffhuber, K.A., Pirrone, N., Ryjkov, A., Selin, N.E., Skov, H., Song, S., Sprovieri, F., Steffen, A., Toyota, K., Travnikov, O., Yang, X., Dommergue, A., 2016. Chemical cycling and deposition of atmospheric mercury in polar regions: review of recent measurements and comparison with models. Atmos. Chem. Phys. 16, 10735–10763.

Ariya, P.A., Dastroor, A.P., Amyot, M., Schroeder, W.H., Barrie, L., Anlauf, K., Raofie, F., Ryzhkov, A., Davignon, D., Lalonde, J., 2004. The Arctic: a sink for mercury. Tellus Ser. B Chem. Phys. Meteorol. 56, 397–403.

Berg, T., Pfaffhuber, K.A., Cole, A.S., Engelsen, O., Steffen, A., 2013. Ten-year trends in atmospheric mercury concentrations, meteorological effects and climate variables at Zeppelin, Ny-Ålesund. Atmos. Chem. Phys. 13, 6575–6586.

Brooks, S.B., Saiz-Lopez, A., Skov, H., Lindberg, S.E., Plane, J.M.C., Goodsite, M.E., 2006. The mass balance of mercury in the springtime arctic environment. Geophys. Res. Lett. 33.

Brosset, C., Iverfeldt, Å., 1989. Interaction of solid gold with mercury in ambient air. Water Air Soil Pollut. 43, 147–168.

Chetelat, J., McKinney, M.A., Amyot, M., Dastoor, A., Douglas, T.A., Heimburger-Boavida, L.E., Kirk, J., Kahilainen, K.K., Outridge, P.M., Pelletier, N., Skov, H., St Pierre, K., Vuorenmaa, J., Wang, F., 2022. Climate change and mercury in the Arctic: abiotic interactions. Sci. Total Environ. 824, 153715.

Cobbett, F.D., Steffen, A., Lawson, G., Van Heyst, B.J., 2007. GEM fluxes and atmospheric mercury concentrations (GEM, RGM and Hgp) in the Canadian Arctic at Alert, Nunavut, Canada (February–June 2005). Atmos. Environ. 41, 6527–6543.

Cole, A.S., Steffen, A., 2010. Trends in long-term gaseous mercury observations in the Arctic and effects of temperature and other atmospheric conditions. Atmos. Chem. Phys. 10, 4661–4672.

Cole, A.S., Steffen, A., Pfaffhuber, K.A., Berg, T., Pilote, M., Poissant, L., Tordon, R., Hung, H., 2013. Ten-year trends of atmospheric mercury in the high Arctic compared to Canadian sub-Arctic and mid-latitude sites. Atmos. Chem. Phys. 13, 1535–1545.

Dastoor, A.P., Durnford, D.A., 2013. Arctic Ocean: is it a sink or a source of atmospheric mercury? Environ. Sci. Technol. 48, 1707–1717.

DiMento, B.P., Mason, R.P., Brooks, S., Moore, C., 2019. The impact of sea ice on the air-sea exchange of mercury in the Arctic Ocean. Deep-Sea Res. I Oceanogr. Res. Pap. 144, 28–38.

Dommergue, A., Sprovieri, F., Pirrone, N., Ebinghaus, R., Brooks, S., Courteaud, J., Ferrari, C.P., 2010. Overview of mercury measurements in the Antarctic troposphere. Atmos. Chem. Phys. 10, 3309–3319.

Douglas, T.A., Blum, J.D., 2019. Mercury isotopes reveal atmospheric gaseous mercury deposition directly to the Arctic coastal snowpack. Environ. Sci. Technol. Lett. 6, 235–242.

Douglas, T.A., Loseto, L.L., Macdonald, R.W., Outridge, P., Dommergue, A., Poulain, A., Amyot, M., Barkay, T., Berg, T., Chételat, J., Constant, P., Evans, M., Ferrari, C., Gantner, N., Johnson, M.S., Kirk, J., Kroer, N., Larose, C., Lean, D., Nielsen, T.G., Poissant, L., Rognerud, S., Skov, H., Sørensen, S., Wang, F., Wilson, S., Zdanowicz, C.M., 2012. The fate of mercury in Arctic terrestrial and aquatic ecosystems, a review. Environ. Chem. 9.

Driscoll, C.T., Mason, R.P., Chan, H.M., Jacob, D.J., Pirrone, N., 2013. Mercury as a global pollutant: sources, pathways, and effects. Environ. Sci. Technol. 47, 4967–4983.

Durnford, D., Dastoor, A., 2011. The behavior of mercury in the cryosphere: a review of what we know from observations. J. Geophys. Res. 116.

Fisher, J.A., Jacob, D.J., Soerensen, A.L., Amos, H.M., Steffen, A., Sunderland, E.M., 2012. Riverine source of Arctic Ocean mercury inferred from atmospheric observations. Nat. Geosci. 5, 499–504.

Fisher, J.A., Jacob, D.J., Soerensen, A.L., Amos, H.M., Corbitt, E.S., Streets, D.G., Wang, Q., Yantosca, R.M., Sunderland, E.M., 2013. Factors driving mercury variability in the Arctic atmosphere and ocean over the past 30 years. Glob. Biogeochem. Cycles 27, 1226–1235.

Fraser, A., Dastoor, A., Ryjkov, A., 2018. How important is biomass burning in Canada to mercury contamination? Atmos. Chem. Phys. 18, 7263–7286.

Gauchard, P., Aspmo, K., Temme, C., Steffen, A., Ferrari, C., Berg, T., Strom, J., Kaleschke, L., Dommergue, A., Bahlmann, E., 2005. Study of the origin of atmospheric mercury depletion events recorded in Ny-Ålesund, Svalbard, spring 2003. Atmos. Environ. 39, 7620–7632.

Gay, D.A., Schmeltz, D., Prestbo, E., Olson, M., Sharac, T., Tordon, R., 2013. The Atmospheric Mercury Network: measurement and initial examination of an ongoing atmospheric mercury record across North America. Atmos. Chem. Phys. 13, 11339–11349.

Gilbert, R.O., 1987. Statistical Methods for Environmental Pollution Monitoring. Wiley.

Goodsite, M.E., Plane, J.M.C., Skov, H., 2004. A theoretical study of the oxidation of Hg0 to HgBr2 in the troposphere. Environ. Sci. Technol. 38, 1772–1776.

Goodsite, M.E., Plane, J.M.C., Skov, H., 2012. Correction to a theoretical study of the oxidation of Hg0 to HgBr2 in the troposphere. Environ. Sci. Technol. 46, 5262.

Gustin, M.S., Huang, J., Miller, M.B., Peterson, C., Jaffe, D.A., Ambrose, J., Finley, B.D., Lyman, S.N., Call, K., Talbot, R., Feddersen, D., Mao, H., Lindberg, S.E., 2013. Do we understand what the mercury speciation instruments are actually measuring? Results of RAMIX. Environ. Sci. Technol. 47, 7295–7306.

Heslin-Rees, D., Burgos, M., Hansson, H.-C., Krejci, R., Ström, J., Tunved, P., Zieger, P., 2020. From a polar to a marine environment: has the changing Arctic led to a shift in aerosol light scattering properties? Atmos. Chem. Phys. 20, 13671–13686.

Hirdman, D., Sodemann, H., Eckhardt, S., Burkhart, J.F., Jefferson, A., Mefford, T., Quinn, P.K., Sharma, S., Ström, J., Stohl, A., 2010. Source identification of short-lived air pollutants in the Arctic using statistical analysis of measurement data and particle dispersion model output. Atmos. Chem. Phys. 10, 669–693.

Horowitz, H.M., Jacob, D.J., Zhang, Y., Dibble, T.S., Slemr, F., Amos, H.M., Schmidt, J.A., Corbitt, E.S., Marais, E.A., Sunderland, E.M., 2017. A new mechanism for atmospheric mercury redox chemistry: implications for the global mercury budget. Atmos. Chem. Phys. 17, 6353–6371.

Huang, M., Carmichael, G.R., Pierce, R.B., Jo, D.S., Park, R.J., Flemming, J., Emmons, L.K., Bowman, K.W., Henze, D.K., Davila, Y., Sudo, K., Jonson, J.E., Lund, M.T., Janssens-Maenhout, G., Dentener, F.J., Keating, T.J., Oetjen, H., Payne, V.H., 2017. Impact of intercontinental pollution transport on North American ozone air pollution: an HTAP phase 2 multi-model study. Atmos. Chem. Phys. 17, 5721–5750.

Iverfeldt, Å., 1991. Mercury in forest canopy throughfall water and its relation to atmospheric deposition. Water Air Soil Pollut. 56, 553–564.

Jiskra, M., Sonke, J.E., Obrist, D., Bieser, J., Ebinghaus, R., Myhre, C.L., Pfaffhuber, K.A., Wängberg, I., Kyllönen, K., Worthy, D., 2018. A vegetation control on seasonal variations in global atmospheric mercury concentrations. Nat. Geosci. 11, 244–250.

Jiskra, M., Sonke, J.E., Agnan, Y., Helmig, D., Obrist, D., 2019. Insights from mercury stable isotopes on terrestrial–atmosphere exchange of Hg(0) in the Arctic tundra. Biogeosciences 16, 4051–4064.

Kamp, J., Skov, H., Jensen, B., Sørensen, L.L., 2018. Fluxes of gaseous elemental mercury (GEM) in the High Arctic during atmospheric mercury depletion events (AMDEs). Atmos. Chem. Phys. 18, 6923–6938.

Landis, M.S., Keeler, G.J., Al-Wali, K.I., Stevens, R.K., 2004. Divalent inorganic reactive gaseous mercury emissions from a mercury cell chlor-alkali plant and its impact on near-field atmospheric dry deposition. Atmos. Environ. 38, 613–622.

Li, P., Peng, C., Wang, M., Li, W., Zhao, P., Wang, K., Yang, Y., Zhu, Q., 2017. Quantification of the response of global terrestrial net primary production to multifactor global change. Ecol. Indic. 76, 245–255.

Lindberg, S.E., Brooks, S., Lin, C.J., Scott, K.J., Landis, M.S., Stevens, R.K., Goodsite, M., Richter, A., 2002. Dynamic oxidation of gaseous mercury in the Arctic troposphere at polar sunrise. Environ. Sci. Technol. 36, 1245–1256.

Lindberg, S., Bullock, R., Ebinghaus, R., Engstrom, D., Feng, X., Fitzgerald, W., Pirrone, N., Prestbo, E., Seigneur, C., 2007. A synthesis of progress and uncertainties in attributing the sources of mercury in deposition. Ambio 19–32.

Lu, J.Y., Schroeder, W.H., Barrie, L.A., Steffen, A., Welch, H.E., Martin, K., Lockhart, L., Hunt, R.V., Boila, G., Richter, A., 2001. Magnification of atmospheric mercury deposition to polar regions in springtime: the link to tropospheric ozone depletion chemistry. Geophys. Res. Lett. 28, 3219–3222.

Lund, M., 2018. Uncovering the unknown—climate interactions in a changing arctic tundra. Environ. Res. Lett. 13, 061001.

Lyman, S.N., Jaffe, D.A., Gustin, M.S., 2010. Release of mercury halides from KCl denuders in the presence of ozone. Atmos. Chem. Phys. 10, 8197–8204.

Lyman, S., Jones, C., O'Neil, T., Allen, T., Miller, M., Gustin, M.S., Pierce, A.M., Luke, W., Ren, X., Kelley, P., 2016. Automated calibration of atmospheric oxidized mercury measurements. Environ. Sci. Technol. 50, 12921–12927.

Ma, J., Hung, H., Tian, C., Kallenborn, R., 2011. Revolatilization of persistent organic pollutants in the Arctic induced by climate change. Nat. Clim. Chang. 1, 255–260.

Macdonald, R.W., Harner, T., Fyfe, J., 2005. Recent climate change in the Arctic and its impact on contaminant pathways and interpretation of temporal trend data. Sci. Total Environ. 342, 5–86.

Martin, L.G., Labuschagne, C., Brunke, E.-G., Weigelt, A., Ebinghaus, R., Slemr, F., 2017. Trend of atmospheric mercury concentrations at Cape Point for 1995–2004 and since 2007. Atmos. Chem. Phys. 17, 2393–2399.

Moore, C.W., Obrist, D., Steffen, A., Staebler, R.M., Douglas, T.A., Richter, A., Nghiem, S.V., 2014. Convective forcing of mercury and ozone in the Arctic boundary layer induced by leads in sea ice. Nature 506, 81–84.

Nguyen, H.T., Kim, K.-H., Shon, Z.-H., Hong, S., 2009. A review of atmospheric mercury in the polar environment. Crit. Rev. Environ. Sci. Technol. 39, 552–584.

Obrist, D., Tas, E., Peleg, M., Matveev, V., Faïn, X., Asaf, D., Luria, M., 2011. Bromine-induced oxidation of mercury in the mid-latitude atmosphere. Nat. Geosci. 4, 22–26.

Obrist, D., Agnan, Y., Jiskra, M., Olson, C.L., Colegrove, D.P., Hueber, J., Moore, C.W., Sonke, J.E., Helmig, D., 2017. Tundra uptake of atmospheric elemental mercury drives Arctic mercury pollution. Nature 547, 201–204.

Obrist, D., Kirk, J.L., Zhang, L., Sunderland, E.M., Jiskra, M., Selin, N.E., 2018. A review of global environmental mercury processes in response to human and natural perturbations: changes of emissions, climate, and land use. Ambio 47, 116–140.

O'Driscoll, N.J., Siciliano, S.D., Peak, D., Carignan, R., Lean, D.R.S., 2006. The influence of forestry activity on the structure of dissolved organic matter in lakes: implications for mercury photoreactions. Sci. Total Environ. 366, 880–893.

Olson, C.L., Jiskra, M., Sonke, J.E., Obrist, D., 2019. Mercury in tundra vegetation of Alaska: spatial and temporal dynamics and stable isotope patterns. Sci. Total Environ. 660, 1502–1512.

Poissant, L., Pilote, M., Constant, P., Beauvais, C., Zhang, H.H., Xu, X., 2004. Mercury gas exchanges over selected bare soil and flooded sites in the bay St. Francois wetlands (Quebec, Canada). Atmos. Environ. 38, 4205–4214.

Poulain, A.J., Garcia, E., Amyot, M., Campbell, P.G.C., Ariya, P.A., 2007. Mercury distribution, partitioning and speciation in coastal vs. inland High Arctic snow. Geochim. Cosmochim. Acta 71, 3419–3431.

Saiz-Lopez, A., Sitkiewicz, S.P., Roca-Sanjuan, D., Oliva-Enrich, J.M., Davalos, J.Z., Notario, R., Jiskra, M., Xu, Y., Wang, F., Thackray, C.P., Sunderland, E.M., Jacob, D.J., Travnikov, O., Cuevas, C.A., Acuna, A.U., Rivero, D., Plane, J.M.C., Kinnison, D.E., Sonke, J.E., 2018. Photoreduction of gaseous oxidized mercury changes global atmospheric mercury speciation, transport and deposition. Nat. Commun. 9, 4796.

Schroeder, W.H., Anlauf, K.G., Barrie, L.A., Lu, J.Y., Steffen, A., Schneeberger, D.R., Berg, T., 1998. Arctic springtime depletion of mercury. Nature 394, 331–332.

Schroeder, W., Anlauf, K., Barrie, L., Steffen, A., Lu, J., 1999. Depletion of mercury vapour in the Arctic troposphere after polar sunrise. WIT Transactions on Ecology and the Environment, p. 36.

Schuster, P.F., Schaefer, K.M., Aiken, G.R., Antweiler, R.C., Dewild, J.F., Gryziec, J.D., Gusmeroli, A., Hugelius, G., Jafarov, E., Krabbenhoft, D.P., Liu, L., Herman-Mercer, N., Mu, C., Roth, D.A., Schaefer, T., Striegl, R.G., Wickland, K.P., Zhang, T., 2018. Permafrost stores a globally significant amount of mercury. Geophys. Res. Lett. 45, 1463–1471.

Selin, N.E., 2009. Global biogeochemical cycling of mercury: a review. Annu. Rev. Environ. Resour. 34, 43–63.

Selin, N.E., Sunderland, E.M., Knightes, C.D., Mason, R.P., 2010. Sources of mercury exposure for US seafood consumers: implications for policy. Environ. Health Perspect. 118, 137–143.

Selyuzhenok, V., Bashmachnikov, I., Ricker, R., Vesman, A., Bobylev, L., 2020. Sea ice volume variability and water temperature in the Greenland Sea. Cryosphere 14, 477–495.

Skov, H., Brooks, S.B., Goodsite, M.E., Lindberg, S.E., Meyers, T.P., Landis, M.S., Larsen, M.R.B., Jensen, B., McConville, G., Christensen, J., 2006. Fluxes of reactive gaseous mercury measured with a newly developed method using relaxed eddy accumulation. Atmos. Environ. 40, 5452–5463.

Skov, H., Hjorth, J., Nordstrøm, C., Jensen, B., Christoffersen, C., Bech Poulsen, M., Baldtzer Liisberg, J., Beddows, D., Dall'Osto, M., Christensen, J.H., 2020. Variability in gaseous elemental mercury at Villum Research Station, Station Nord, in North Greenland from 1999 to 2017. Atmos. Chem. Phys. 20, 13253–13265.

Sonke, J.E., Teisserenc, R., Heimbürger-Boavida, L.-E., Petrova, M.V., Marusczak, N., Le Dantec, T., Chupakov, A.V., Li, C., Thackray, C.P., Sunderland, E.M., 2018. Eurasian river spring flood observations support net Arctic Ocean mercury export to the atmosphere and Atlantic Ocean. Proc. Natl. Acad. Sci. 115, E11586–E11594.

Sprovieri, F., Pirrone, N., Ebinghaus, R., Kock, H., Dommergue, A., 2010. A review of worldwide atmospheric mercury measurements. Atmos. Chem. Phys. 10, 8245–8265.

Steen, A.O., Berg, T., Dastoor, A.P., Durnford, D.A., Engelsen, O., Hole, L.R., Pfaffhuber, K.A., 2011. Natural and anthropogenic atmospheric mercury in the European Arctic: a fractionation study. Atmos. Chem. Phys. 11, 6273–6284.

Steffen, A., Schroeder, W., Bottenheim, J., Narayan, J., Fuentes, J.D., 2002. Atmospheric mercury concentrations: measurements and profiles near snow and ice surfaces in the Canadian Arctic during Alert 2000. Atmos. Environ. 36, 2653–2661.

Steffen, A., Schroeder, W.H., Edwards, G., Banic, C., 2003. Mercury Throughout Polar Sunrise 2002. EDP sciences, pp. 1267–1270.

Steffen, A., Schroeder, W., Macdonald, R., Poissant, L., Konoplev, A., 2005. Mercury in the Arctic atmosphere: an analysis of eight years of measurements of GEM at Alert (Canada) and a comparison with observations at Amderma (Russia) and Kuujjuarapik (Canada). Sci. Total Environ. 342, 185–198.

Steffen, A., Douglas, T., Amyot, M., Ariya, P., Aspmo, K., Berg, T., Bottenheim, J., Brooks, S., Cobbett, F., Dastoor, A., Dommergue, A., Ebinghaus, R., Ferrari, C., Gardfeldt, K., Goodsite, M.E., Lean, D., Poulain, A.J., Scherz, C., Skov, H., Sommar, J., Temme, C., 2008. A synthesis of atmospheric mercury depletion event chemistry in the atmosphere and snow. Atmos. Chem. Phys. 8, 1445–1482.

Steffen, A., Bottenheim, J., Cole, A., Douglas, T.A., Ebinghaus, R., Friess, U., Netcheva, S., Nghiem, S., Sihler, H., Staebler, R., 2013. Atmospheric mercury over sea ice during the OASIS-2009 campaign. Atmos. Chem. Phys. 13, 7007–7021.

Steffen, A., Bottenheim, J., Cole, A., Ebinghaus, R., Lawson, G., Leaitch, W.R., 2014. Atmospheric mercury speciation and mercury in snow over time at Alert, Canada. Atmos. Chem. Phys. 14, 2219–2231.

Steffen, A., Lehnherr, I., Cole, A., Ariya, P., Dastoor, A., Durnford, D., Kirk, J., Pilote, M., 2015. Atmospheric mercury in the Canadian Arctic. Part I: a review of recent field measurements. Sci. Total Environ. 509–510, 3–15.

Stern, G.A., Macdonald, R.W., Outridge, P.M., Wilson, S., Chetelat, J., Cole, A., Hintelmann, H., Loseto, L.L., Steffen, A., Wang, F., Zdanowicz, C., 2012. How does climate change influence Arctic mercury? Sci. Total Environ. 414, 22–42.

Streets, D.G., Horowitz, H.M., Jacob, D.J., Lu, Z., Levin, L., Ter Schure, A.F.H., Sunderland, E.M., 2017. Total mercury released to the environment by human activities. Environ. Sci. Technol. 51, 5969–5977.

Streets, D.G., Horowitz, H.M., Lu, Z., Levin, L., Thackray, C.P., Sunderland, E.M., 2019. Global and regional trends in mercury emissions and concentrations, 2010–2015. Atmos. Environ. 201, 417–427.

Sunderland, E.M., Krabbenhoft, D.P., Moreau, J.W., Strode, S.A., Landing, W.M., 2009. Mercury sources, distribution, and bioavailability in the North Pacific Ocean: insights from data and models. Glob. Biogeochem. Cycles 23.

Toyota, K., McConnell, J.C., Staebler, R.M., Dastoor, A.P., 2014. Air–snowpack exchange of bromine, ozone and mercury in the springtime Arctic simulated by the 1-D model PHANTAS–part 1: in-snow bromine activation and its impact on ozone. Atmos. Chem. Phys. 14, 4101–4133.

Wang, S., McNamara, S.M., Moore, C.W., Obrist, D., Steffen, A., Shepson, P.B., Staebler, R.M., Raso, A.R.W., Pratt, K.A., 2019. Direct detection of atmospheric atomic bromine leading to mercury and ozone depletion. Proc. Natl. Acad. Sci. U. S. A. 116, 14479–14484.

Weigelt, A., Ebinghaus, R., Manning, A.J., Derwent, R.G., Simmonds, P.G., Spain, T.G., Jennings, S.G., Slemr, F., 2015. Analysis and interpretation of 18 years of mercury observations since 1996 at Mace Head, Ireland. Atmos. Environ. 100, 85–93.

Weiss-Penzias, P.S., Gay, D.A., Brigham, M.E., Parsons, M.T., Gustin, M.S., Ter Schure, A., 2016. Trends in mercury wet deposition and mercury air concentrations across the U.S. and Canada. Sci. Total Environ. 568, 546–556.

Yang, X., Pyle, J.A., Cox, R.A., 2008. Sea salt aerosol production and bromine release: role of snow on sea ice. Geophys. Res. Lett. 35.

Yang, X., Blechschmidt, A.-M., Bognar, K., McClure-Begley, A., Morris, S., Petropavlovskikh, I., Richter, A., Skov, H., Strong, K., Tarasick, D.W., 2020. Pan-Arctic surface ozone: modelling vs. measurements. Atmos. Chem. Phys. 20, 15937–15967.

Zhang, L., Wright, L.P., Blanchard, P., 2009. A review of current knowledge concerning dry deposition of atmospheric mercury. Atmos. Environ. 43, 5853–5864.

Zhang, Y., Jacob, D.J., Dutkiewicz, S., Amos, H.M., Long, M.S., Sunderland, E.M., 2015. Biogeochemical drivers of the fate of riverine mercury discharged to the global and Arctic oceans. Glob. Biogeochem. Cycles 29, 854–864.

Zheng, W., Chandan, P., Steffen, A., Stupple, G., De Vera, J., Mitchell, C.P.J., Wania, F., Bergquist, B.A., 2021. Mercury stable isotopes reveal the sources and transformations of atmospheric Hg in the high Arctic. Appl. Geochem. 131.